N78-70355

Accession No. 86086-64

Copy No. SID 64-1563

HIGH-VACUUM PLUME IMPINGEMENT TEST CORRELATION

NAS9-150

August 1964

Exhibit I, Paragraph 5.5

NORTH AMERICAN AVIATION, INC.
SPACE and INFORMATION SYSTEMS DIVISION

FOREWORD

This report was prepared by E. T. Piesik of the Propulsion Analysis section of Apollo Engineering, Space and Information Systems Division, North American Aviation, Inc. The encouragement and technical assistance of R. R. Koppang, Supervisor, and D. J. Simkin, Chief, Propulsion Analysis, are gratefully acknowledged.

ABSTRACT

A method is described and equations are presented which are sufficient to determine the over-all surface heating rates and pressures on a flat plate due to highly underexpanded rocket exhaust impingement. The results are compared to centerline test data obtained from the Apollo service module RCS high-vacuum plume impingement test at Arnold Engineering Development Center (AEDC). It is also demonstrated that, for sufficiently underexpanded exhaust flows, the results are directly applicable over a large range of total-to-ambient pressure ratios, including space conditions. This method has been used to determine heating rates on the Apollo service module due to plume impingement from the service module RCS pitch and yaw engines.

CONTENTS

ILLUSTRATIONS

TABLES

INTRODUCTION

The reaction control system (RCS) rocket engines on the Apollo spacecraft are placed on the service module in such a manner that the effects of engine exhaust plume impingement on the vehicle (surface heating and surface pressure) are important to structural integrity. In order to determine experimentally the amount of thermal protection required on the service module because of plume impingement heating, a series of tests was performed in the AEDC J2A test cell from March through May of 1963. These tests are described fully in the "High-Vacuum Plume Impingement Test Report," SID 63-1520.[1] Sufficient parametric data were obtained from the tests to allow a theoretical correlation of the results.

The purpose of this report is to present analytical methods (backed up by experimental data) for predicting the heating rates and surface pressures which result from an exhaust plume impinging on a flat plate in space. These methods have been used to design the service module plume heat shields for the roll, pitch, and yaw RCS engines.

[1] Reference 1

HIGHLY EXPANDED EXHAUST FLOW FIELDS

In a space environment, the flow from a rocket nozzle expands around the nozzle lip to a maximum value according to a Prantl-Meyer expansion. Depending on the specific heat ratio of the gas and the Mach number of the nozzle exit, the flow turning angle of the gas may well exceed 90 degrees, and exhaust impingement on nearby vehicle structure will occur. Theoretical predictions of the effects of this impingement require that the internal and external nozzle flow fields and the properties on the impinged surface be known. The technique for determining the properties of the undisturbed exhaust flow field utilizes hyperbolic nonlinear equations of motion for two-dimensional nonviscous irrotational flow. These are most easily solved by the method of characteristics.[1] These calculations require an accurate knowledge of the conditions of the flow (flow field distribution and thermodynamic properties) at the nozzle exit plane.

In order to determine the exact exhaust flow field, the source of the flow and all conditions leading up to the flow field must be considered. The chemical products of combustion, the temperature, and the pressure must be known throughout the nozzle and the plume flow fields. Of course the specific heat ratio of the gas varies continually from the chamber downstream throughout the exhaust flow field. For complex throat and nozzle contours, the flow must be considered in three dimensions in order to determine the shock formation and flow field. The shock formation in the nozzle will also propagate into the plume. There is no boundary shock for a plume in space, unlike the low-altitude condition where the flow is compressed back to ambient pressure.

The method of characteristics is capable of solving such a complex problem and accounting for a variable specific heat ratio (dependent upon chemical composition and static temperature) and shock formation with attendant entropy change. Individual computer programs exist at S&ID and throughout industry which calculate various parts of the problem: chemical composition and engine performance parameters at various nozzle area ratios, three-dimensional nozzle characteristic flow field properties with variable specific heat ratio for performance loss calculations (usually not accounting for shock formation), and exhaust plume flow field characteristics based on the nozzle exit Mach number and exit pressure (usually at a constant

[1] Reference 2

specific heat ratio and accounting only for the boundary shock). The author does not know of a computer program which currently accounts for all physical phenomena which make up the exhaust flow field of a contoured nozzle rocket engine. Because of the complexity of calculating plume flow fields for other than relatively simple nozzle exit conditions, the requirements for an exact flow field calculation must usually be relaxed. Nevertheless it will be shown, at least for the engine tested, that a very simple analysis of the exhaust flow field will result in good correlation with the experimental data on heating rate and surface pressure for a flat plate impinged upon by an exhaust plume in a near-perfect vacuum.

CONSTANT FLOW PROPERTIES

Theoretically, the method of characteristics shows that nondimensional plume flow field properties, iso-Mach lines, and streamlines do not vary inside the boundary shock over a large range of ambient-to-total chamber pressure ratios (for a particular nozzle and specific heat ratio). The explanation is that the flow field is supersonic, and downstream effects cannot propagate upstream. Absolute properties, of course, vary with combustion chamber properties.

The question remains as to whether local properties inside the boundary shock on an interfering surface will be substantially affected by a change in ambient pressure. If local impingement properties are unaffected, the required space data may be obtained in available test chambers with altitude capabilities of 200,000 to 400,000 feet.

Bauer and Schlumpf of AEDC[1] studied surface pressures experimentally from a plume impinging on a flat plate at pressure ratios (P_t/P_∞) from 2×10^3 to 1.4×10^4. Vick of Langley Research Laboratories[2] covered the P_t/P_∞ range from 5×10^4 to 2.5×10^5. The "High-Vacuum Plume Impingement Test Report"[3] covered the P_t/P_∞ range from 10^4 to 10^8. Additional information is reported by Margolin and Welch[4] for a P_t/P_∞ range from 1×10^3 to 2.3×10^3.

The experimental results cover cold inert gases, typical rocket engine combustion products, conical and contoured nozzles, various area ratios (1 to 40), and a wide range of P_t/P_∞ (10^3 to 10^8). For each experimental configuration, the impingement pressure ratio (P_s/P_t) at any particular location on the test surface inside the boundary shock is essentially invariant (±10 percent) with P_t/P_∞. The variation has neither trend nor consistency and can probably be attributed to experimental error.

The preponderance of experimental data shows that over a very broad range of total-to-ambient pressure ratios ($P_t/P_\infty = 10^3$ to 10^8), the surface-to-total pressure ratio (P_s/P_t) at a point inside the boundary shock is essentially invariant with P_t/P_∞ for any particular nozzle and surface configuration.

---

[1]Reference 3
[2]Reference 4
[3]Reference 1
[4]Reference 5

Additional evidence is presented in the "High-Vacuum Plume Impingement Test Report"[1] to show that the ambient pressure does not significantly influence the surface properties internal to the plume boundary shock. Temperature-time histories of thin-skin thermocouples which have essentially constant slopes (constant heating rates) are presented. If the local properties (M_2, T_2, P_2) were changing, then the heating rate would also change.

With the above evidence accepted, it appears that results of plume impingement tests performed at less than a space condition are also valid in space if the data inside the boundary shock region are used.

[1]Reference 1

TEST PROGRAM

A complete description of the Apollo service module RCS plume impingement test with a flat plate surface is given in the "High-Vacuum Plume Impingement Test Report"[1] along with a considerable amount of the test results; a short description is included here.

A prototype service module RCS engine with a parabolic 40:1 area ratio nozzle and three nozzles of the same contour, truncated at area ratios of 20:1, 15:1, and 10:1, was fired in the J2A test cell at AEDC. The altitude varied during the engine firings from 400,000 feet to 200,000 feet in 2 seconds. The rocket engines used Aerozine-50 (50 percent hydrazine [N_2H_4] and 50 percent unsymmetrical dimethyl hydrazine [UDMH]), and nitrogen tetroxide (N_2O_4) at a nominal mixture ratio of 2.0 and chamber pressure of 90 psia. The throat diameter of the engine was 0.868 inches.

The test panel was fabricated of 0.008-inch stainless steel skin on a flat 6-foot-by-6 foot aluminum honeycomb support panel. The panel was positioned at various standoff distances to the nozzle centerline and with various nozzle centerline-to-plate cant angles. The matrix of nozzle area ratios, standoff distance, and cant angles is given in Table 1. 75 thermocouples and 36 pressure transducers were located on the stainless steel skin as shown in Figures 1 and 2. Surface pressures were obtained directly from the pressure transducer readout. Heating rates were obtained from the temperature-time histories using the "thin-skin" equation and an average heat capacity for the stainless steel. As stated in SID 63-1520,[1] the heating rate test data accuracy is considered to be ±10% or 0.1 Btu/ft^2/sec, whichever is greater.

[1] Reference 1

Table 1. Test Run Schedule

Data Point	Plate Elevation h (R_e)	Plate Cant Angle δ (deg)	Fuel Flow Rate (lb/sec)	Oxidizer Flow Rate (lb/sec)	Mixture Ratio	Injector Face Chamber Pressure P_c (psia)	Exit Pressure P_{ex} (psia)
ε = 40:1, RUN 01							
20	10.7	0	0.1143	No data	No data	98	Not instrumented
21	10.7	0	0.1215	↓	↓	99	↓
22	10.7	0	0.1103			97	
23	10.7	0	0.1080			97	
24	10.7	0	0.1098			98	
35	3.0	0	0.1098			97	
36	3.0	0	0.1134			98	
37	7.0	0	0.1139			97	
38	7.0	0	0.1103			97	
39	10.7	0	0.1103			98	
40	10.7	0	0.1114			98	
ε = 40:1, RUN 01A							
20	3.0	0	0.113	0.241	2.13	97	Not instrumented
21	3.0	0	0.116	0.235	2.04	97	↓
22	3.0	10	0.112	0.238	2.13	96	
23	3.0	10	0.112	0.237	2.12	97	
24	3.0	15	0.112	0.237	2.11	96	
25	3.0	15	0.114	0.237	2.08	97	
36	3.0	25	0.128	0.236	1.84	96	
37	3.0	25	0.110	0.239	2.17	97	
38	3.0	35	0.109	0.237	2.18	96	
39	3.0	35	0.116	0.237	2.04	96	
40	7.0	0	0.111	0.234	2.10	97	
41	7.0	15	0.116	0.235	2.03	101	
42	7.0	25	0.105	0.235	2.23	96	
53	10.7	0	0.114	0.240	2.11	96	
54	10.7	15	0.116	0.234	2.02	96	
55	10.7	15	0.112	0.234	2.09	96	
56	10.7	0	0.112	0.235	2.09	96	
57	7.0	0	0.113	0.235	2.08	95	
58	7.0	15	0.116	0.229	1.98	96	
59	7.0	25	0.113	0.230	2.03	96	
ε = 20:1, RUN 02							
20	3.0	0	0.119	0.247	2.08	95	0.69
21	3.0	0	0.111	0.245	2.21	96	0.73
22	3.0	15	0.111	0.241	2.18	95	0.72
23	3.0	15	0.111	0.241	2.17	95	0.73
24	3.0	25	0.110	0.241	2.20	96	0.73
25	3.0	25	0.110	0.240	2.18	96	0.73
36	7.0	0	No data	No data	No data	96	0.73

Table 1. Test Run Schedule (Cont)

Data Point	Plate Elevation h (R_e)	Plate Cant Angle δ (deg)	Fuel Flow Rate (lb/sec)	Oxidizer Flow Rate (lb/sec)	Mixture Ratio	Injector Face Chamber Pressure P_c (psia)	Exit Pressure P_{ex} (psia)
37	7.0	15	No data	No data	No data	97	0.73
38	7.0	25				96	0.72
39	7.0	35				96	0.72
40	11.0	0				96	0.73
41	11.0	15				96	0.73
42	11.0	25				96	0.73
43	11.0	35				95	0.70
54	11.0	35				96	0.72
55	15.0	0				96	0.65
56	15.0	0	Ran out of propellant			35	0.25
			ϵ = 15:1, RUN 03				
20	12.8	35	0.102	0.249	2.44	92	0.93
21	↓	35	0.103	0.244	2.37	93	0.93
22		25	0.106	0.244	2.30	93	0.94
23		25	0.106	0.237	2.24	91	0.94
24		15	0.106	0.224	2.11	91	0.93
25		15	0.109	0.221	2.02	91	0.93
26		0	0.109	0.221	2.02	91	0.94
27	12.8	0	0.110	0.221	2.01	92	0.93
38	9.0	35	0.102	0.211	2.07	91	0.93
39	↓	35	0.101	0.208	2.06	91	0.93
40		25	0.110	0.220	2.00	91	0.93
41		25	0.110	0.220	2.00	91	0.93
42		15	0.104	0.213	2.04	91	0.93
43		15	0.110	0.221	2.00	91	0.93
44		0	0.110	0.221	2.00	91	0.94
45	9.0	0	0.110	0.221	2.00	91	0.96
57	7.0	35	0.111	0.223	2.00	91	0.95
58	↓	35	0.101	0.222	2.20	91	0.96
59		25	0.110	0.217	1.97	91	0.96
60		25	0.107	0.222	2.07	91	0.95
61		15	0.110	0.222	2.02	91	0.96
62		15	0.109	0.221	2.04	91	0.96
63		0	0.109	0.222	2.04	91	0.95
64	7.0	0	No data	No data	No data	91	0.95
76	5.0	35	0.110	0.221	2.01	92	0.95
77	↓	35	0.110	0.221	2.01	91	0.96
78		25	0.110	0.221	2.01	91	0.96
79		25	0.110	0.221	2.01	91	0.96
80		15	0.110	0.221	2.01	91	0.95
81		15	0.110	0.220	2.00	91	0.95
82		0	0.110	0.221	2.01	92	0.96
83		0	0.110	0.222	2.02	91	0.95
84	5.0	0	0.104	0.222	2.07	—	0.96

Table 1. Test Run Schedule (Cont)

Data Point	Plate Elevation h (R_e)	Plate Cant Angle δ (deg)	Fuel Flow Rate (lb/sec)	Oxidizer Flow Rate (lb/sec)	Mixture Ratio	Injector Face Chamber Pressure P_c (psia)	Exit Pressure P_{ex} (psia)
ϵ = 10:1, RUN 04							
58	11.0	35	0.115	0.188	1.63	83	No data
59		35	0.112	0.200	1.78	85	
60		25	0.113	0.194	1.70	84	
61		25	0.113	0.200	1.78	86	
62		15	0.106	0.198	1.86	87	
63		15	0.112	0.207	1.85	89	
64		0	0.114	0.210	1.84	89	
65	11.0	0	0.109	0.206	1.88	88	
76	7.0	35	0.108	0.226	2.10	90	
77		35	0.107	0.222	2.07	90	
78		25	0.109	0.221	2.02	90	
79		25	0.110	0.225	2.04	90	
80		15	0.109	0.223	2.04	90.	
81		15	0.110	0.224	2.05	90	
82		0	0.109	0.224	2.05	90	
83		0	0.109	0.224	2.05	90	
95		0	0.109	0.216	1.98	88	
96	7.0	0	0.111	0.221	2.00	89	
ϵ = 10:1, RUN 04A							
20	5.0	35	0.104	0.218	2.09	88	1.62
21		35	0.110	0.208	1.89	89	1.62
22		25	0.110	0.207	1.87	—	1.62
23		25	0.109	0.206	1.89	89	1.64
24		15	0.109	0.209	1.92	89	1.64
25		15	0.109	0.207	1.90	89	1.64
26		0	0.108	0.208	1.93	89	1.62
27	5.0	0	0.110	0.212	1.93	89	1.64
38	3.0	35	0.108	0.195	1.80	89	1.66
39		35	0.109	0.206	1.90	89	1.69
40		25	0.110	0.213	1.94	89	1.67
41		25	0.112	0.217	1.95	88	1.67
42		15	0.111	0.217	1.95	88	1.68
43		15	0.109	0.215	1.96	89	1.68
44		0	0.109	0.229	2.10	89	1.68
45	3.0	0	0.110	0.215	1.96	88	1.68
56	9.0	35	0.110	0.215	1.96	88	1.64
57		35	0.108	0.215	1.99	88	1.65
58		25	0.100	0.214	2.14	89	1.63
59		25	0.109	0.215	1.98	88	1.64
60		15	0.111	0.216	1.94	90	1.68
61	9.0	15	0.111	0.216	1.94	90	1.66

Table 1. Test Run Schedule (Cont)

Data Point	Plate Elevation h (R_e)	Plate Cant Angle δ(deg)	Fuel Flow Rate (lb/sec)	Oxidizer Flow Rate (lb/sec)	Mixture Ratio	Face Chamber Pressure P_c (psia)	Exit Pressure P_{ex} (psia)
62	9.0	0	0.113	0.216	1.91	91	1.68
63	9.0	0	0.113	0.215	1.91	91	1.68
74	13.0	35	0.111	0.221	1.99	92	1.70
75	↓	35	0.113	0.220	1.95	92	1.68
76	↓	25	0.112	0.221	1.98	92	1.70
77	↓	25	0.112	0.221	1.98	92	1.68
78	↓	15	0.116	0.228	1.97	92	1.69
79	↓	15	0.113	0.224	1.98	91	1.66
82	↓	0	No data	No data	No data	90	1.66
84	13.0	0	↓	↓	↓	90	1.65
85	17.5	0	↓	↓	↓	90	1.65
86	17.5	0	↓	↓	↓	90	1.70

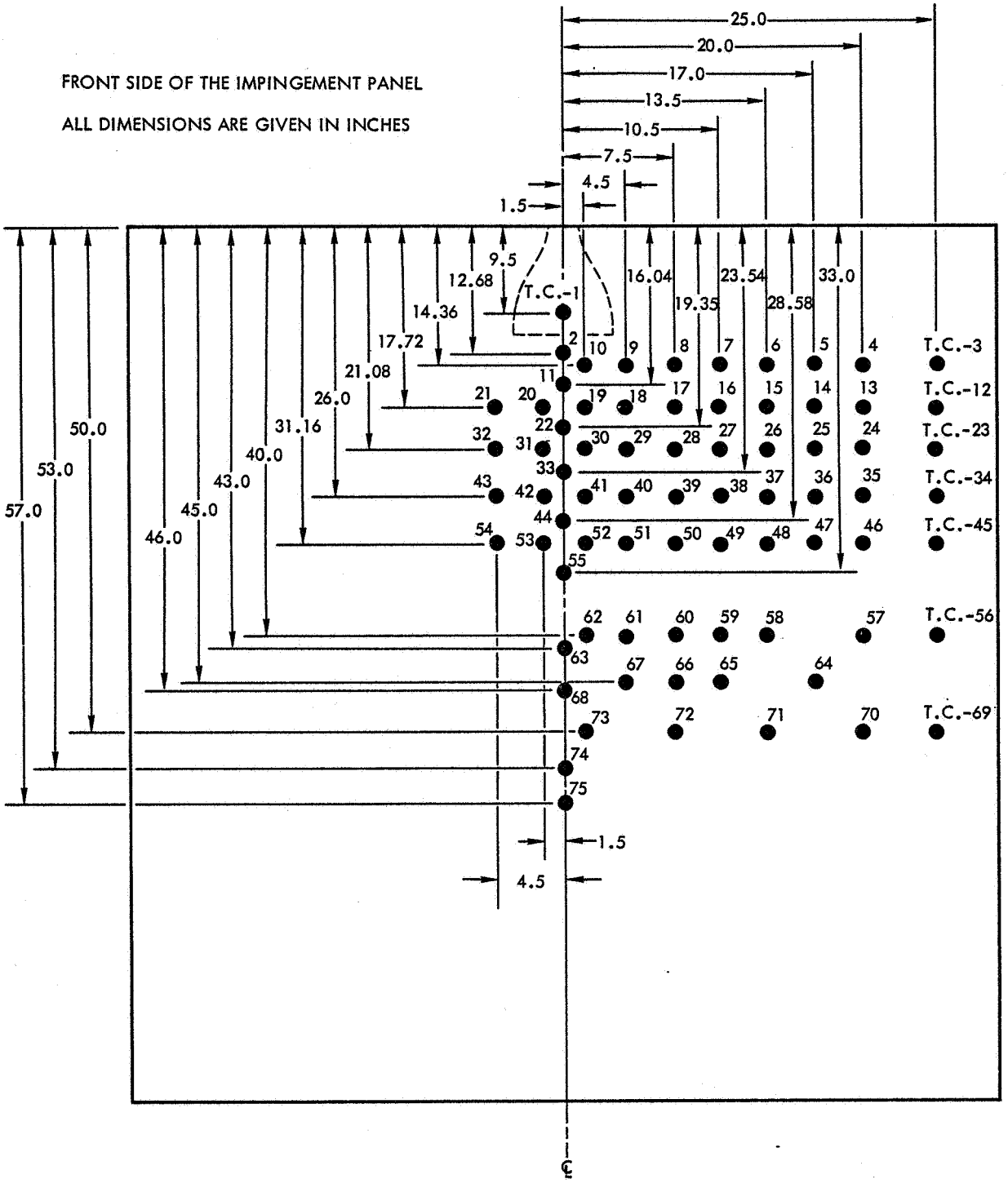

Figure 1. Thermocouple Locations

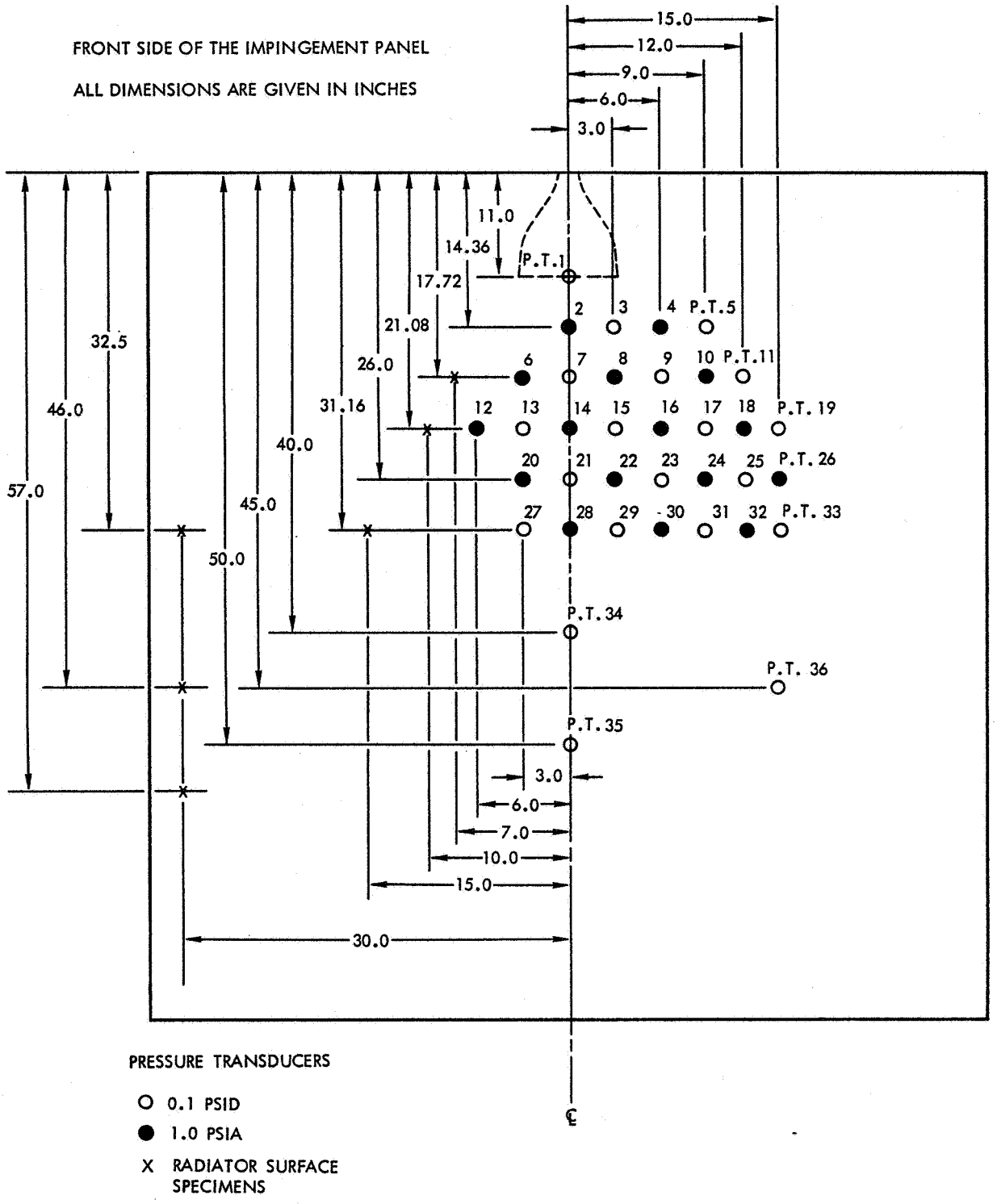

Figure 2. Pressure Transducer Locations

APPROXIMATE EXHAUST FLOW FIELD

Before a prediction can be made of the effects on a surface due to an impinging plume, the external exhaust flow field must be established. A prerequisite for establishing this flow field by the method of characteristics is a knowledge of the thermodynamic properties and the flow field at the nozzle exit plane. The conditions at the nozzle exit plane are established through a combination of measured engine performance data and a theoretical one-dimensional performance program. The program is based on one-dimensional nozzle flow with shifting equilibrium to the throat and frozen flow thereafter. The I_{sp}, ratio of specific heat, pressure ratio, and temperature are obtained from the program at the exit plane of the engine operating at the nominal mixture ratio. The absolute exit plane properties are obtained as follows:

1. Exit ratio of specific heat: directly from program

2. Effective exit static pressure: from the chamber pressure input to the performance program and the exit pressure ratio output

$$P_e = \frac{P_t}{\left(\frac{P_t}{P_e}\right)_{1D}} \tag{1}$$

3. Effective exit temperature: from measured C* efficiency of the engine and the theoretical exit static temperature

$$T_e = (\zeta_{C^*})^2 T_s \tag{2}$$

4. Effective exit Mach number: from the estimated vacuum specific impulse and the effective static exit temperature (It should be noted that the flow chemistry is frozen well upstream of the nozzle exit.)

$$M_e = \frac{V_e}{a_e} = \frac{g\,(I_{sp} - P_e\,A_e/\dot{W})}{(\gamma_e\, g\, R\, T_e)^{1/2}} \tag{3}$$

The total pressure used in the flow field calculations is different from the chamber pressure input to the performance program, but is consistent with the exit properties and the exit specific heat ratio. This effective total pressure is calculated using the effective exit pressure, equation (1), and a one-dimensional isentropic pressure ratio based on the effective exit Mach number, equation (3), and the exit ratio of specific heats.

$$P_t = \left(\frac{P_t}{P_e}\right)_{\gamma_e} P_e \qquad (4)$$

The effective total pressure is a fictitious value. However, the exit properties calculated above are the average bulk properties of the actual flow through the nozzle exit plane and hence yield the actual engine mass flow rate. It is felt that the static pressure and the mass flow rate at the exit more strongly influence the exhaust plume mass flux distribution and, therefore, the impingement heat flux calculations. For this reason, it was considered important to obtain realistic values at the exit plane.

The above properties are required in the input of the method-of-characteristics program which will accept only constant exit plane properties. The space exhaust flow fields calculated for three of the four nozzles used in this test series are presented in Figures 3 to 5. The boundary of the flow field in space is calculated by the Prantl-Meyer expansion. In a test chamber where the ambient pressure is known, the exhaust flow boundary (and boundary shock region) is calculated by the characteristics program using the actual ambient pressure and the effective total pressure.

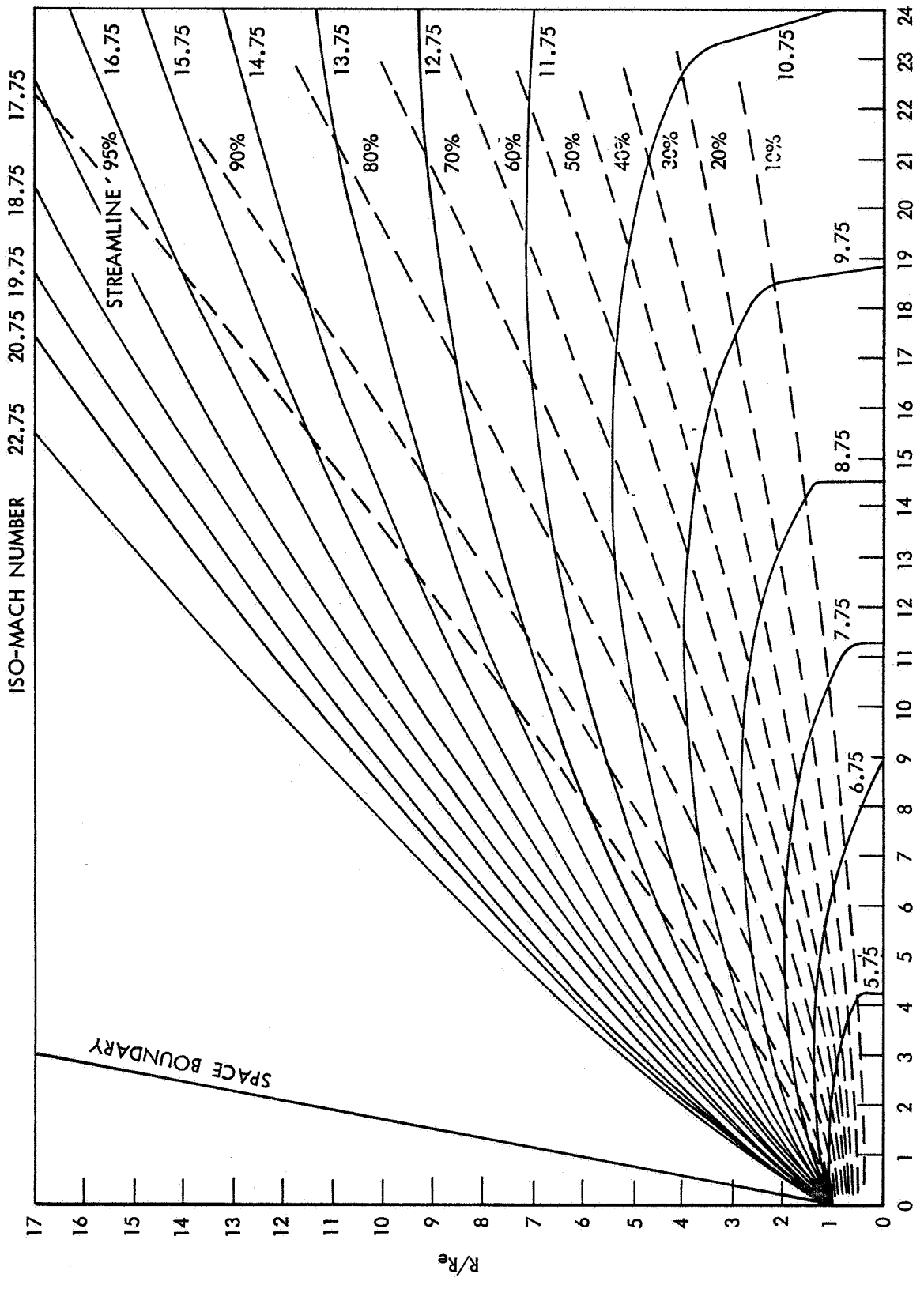

Figure 3. Service Module RCS Space Plume, $\epsilon = 40$

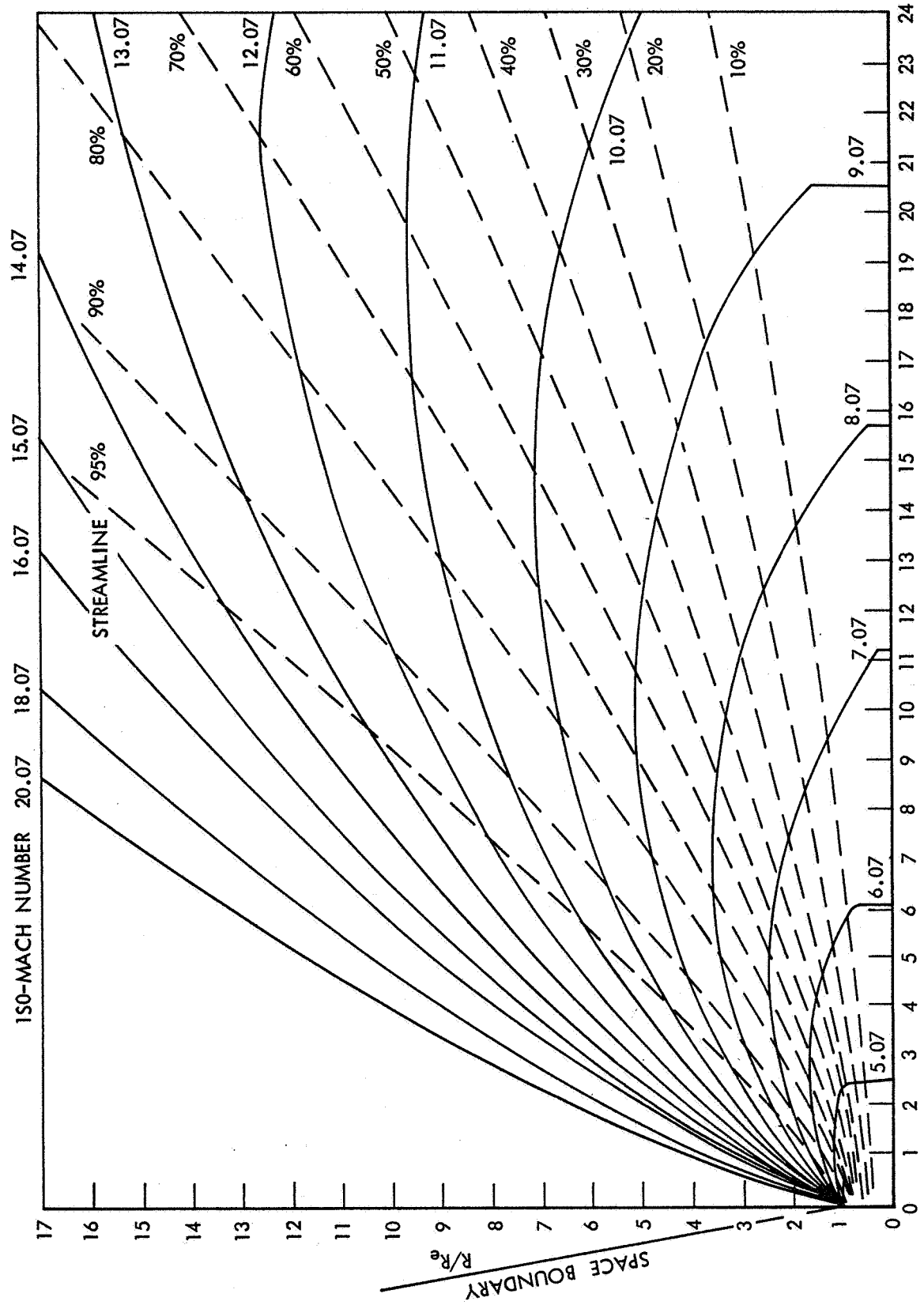

Figure 4. Service Module RCS Space Plume, $\epsilon = 20$

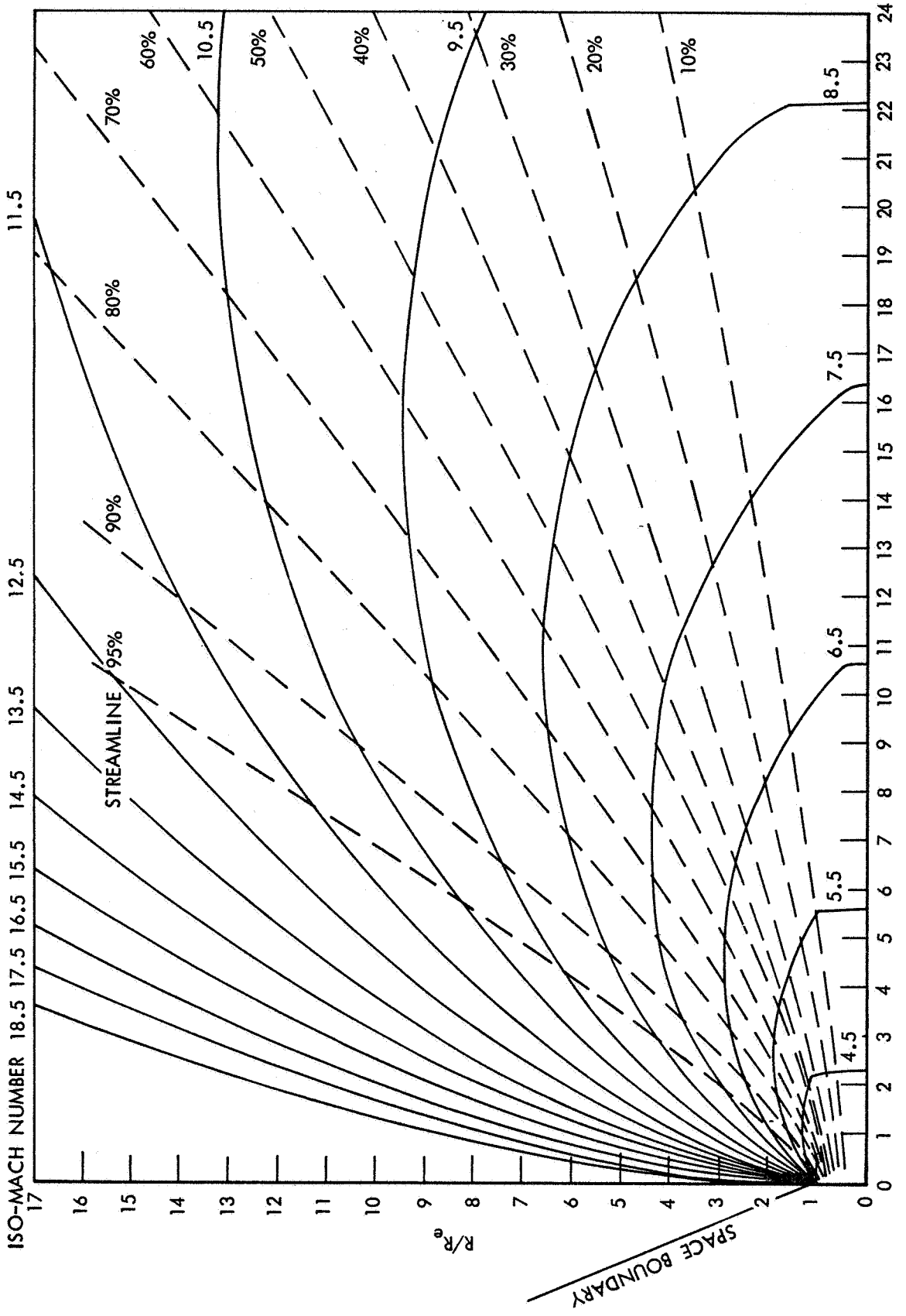

Figure 5. Service Module RCS Space Plume, $\epsilon = 10$

PREDICTION OF HEATING RATES AND SURFACE PRESSURES

From the exhaust flow fields, the upstream property values of Mach number and streamline angle can be obtained at any point of interest on the surface (a flat plate in the present case). It is necessary to obtain the true impingement angle of the flow at the surface, and the local values of surface pressure, density, and velocity. Depending on the specific heat ratio, the true impingement angle, and the upstream Mach number at the point of interest, the flow will be compressed on the surface through either a normal or an oblique shock. A computer program has been developed which takes the output of the exhaust flow field program and the position of the surface in the flow field and computes local values of true impingement angle, Mach number, temperatures, isentropic pressure, and Newtonian pressure assuming that the plume flow field is undistorted (i.e., hypersonic flow approximation). These values are based upon the ratio of specific heats at the nozzle exit.

As stated above, the surface pressures in the oblique shock region are obtained directly from the computer. The equations used are as follows:

Isentropic flow:

$$P_s = \frac{P_2}{P_1} \times \frac{P_1}{P_t} \times P_t \tag{5}$$

Newtonian flow:

$$P_s = \left(\gamma M_1^2 \sin^2 \alpha - 1\right) \frac{P_1}{P_t} \times P_t \tag{6}$$

where P_2/P_1 is the static pressure ratio through the oblique shock, P_1/P_t is the pressure ratio at the impingement Mach number (M_1) before the shock, P_t is given by equation (4), and α is the streamline impingement angle.

The local temperatures in the oblique shock region were obtained from the computer using the following:

$$T_2 = \frac{T_2}{T_1} \times \frac{T_1}{T_t} \times T_t \tag{7}$$

where T_2/T_1 is the static temperature ratio through the oblique shock, T_1/T_t is the temperature ratio at the impingement Mach number before the shock, and T_t is given by equation (9).

In the normal shock region pressure and temperatures were hand computed:

Pressure:

$$P_s = \frac{P_{t_2}}{P_{t_1}} \times P_{t_1} \tag{8}$$

where P_{t_2}/P_{t_1} is the total pressure ratio at the impingement Mach number before the shock, and P_{t_1} is the total pressure of equation (4).

Temperature:

$$T_t = \frac{T_t}{T_e} \times T_e \tag{9}$$

where T_t/T_e is the temperature ratio at the nozzle exit and T_e is obtained from equation (2).

The total temperature is different from that calculated in the engine chamber by the performance computer program, but it is consistent with the nozzle exit γ, M_e, and T_e used to derive the exhaust flow field.

CORRELATING EQUATIONS

HEATING RATE, NORMAL SHOCK REGION

The correlating predictions of heating rates were calculated separately for the normal and the oblique shock region. For the normal shock region, it was convenient to adapt Kemp and Riddel's empirical satellite reentry heating equation.[1] The basic structure of the equation was retained, but a new constant was empirically determined. It was also found necessary to change the body dimension parameter (R) to one relating to the engine and test configuration, because the flow field is smaller than the body being impinged upon. Hence, its dimensions control the shock structure and boundary layer properties on the plate. The equation has been nondimensionalized on the sea-level density of air and the maximum velocity obtainable by expanding the flow to zero absolute temperature. The final form for this empirical equation is as follows:

$$q_{conv} = \frac{15,200}{\epsilon + \frac{0.75\,h}{R_e}} \left(\frac{\rho}{\rho_{SL}}\right)^{1/2} \left(\frac{V}{V_M}\right)^{3.25} \left(1 - \frac{H_W}{H}\right) \text{(Btu/ft}^2\text{/sec)} \qquad (10)$$

where ρ and V are the undisturbed flow field values at the point of interest, and ρ is obtained from the following:

$$\rho = \frac{\rho}{\rho_t} \times \frac{\rho_t}{\rho_e} \times \rho_e \qquad (11)$$

The exit density must be used to maintain the flow field consistency with exit plane properties.

HEATING RATE, OBLIQUE SHOCK REGION

Boundary layer transition was investigated for both momentum and displacement thickness as the distance term in the Reynolds number, and the entire test plate was found to be laminar.

Plume impingement data are presented by Walker, Pratt, and Gaudmight,[2] correlated in the slip flow regime. For the present test, the Knudsen number criteria based on momentum or the displacement thickness

[1] Reference 6
[2] Reference 7

of the boundary layer indicate that the exhaust flow is in the slip flow or transition flow regime. The flat plate used in this test is of the same order as the size of the flow field diameter. If a body dimension is used, the Knudsen number criterion indicates a continuous flow regime. It was assumed in this correlation that the flow was continuous. As will be seen in the Results section, the correlation with a continuous flow assumption is very good.

In the oblique shock region an approximation to the laminar Van Driest equation[1] was used to correlate the heating rate data.

$$q_{conv} = \frac{1.49 \times 10^{-9}}{\rho_{SL}^{1/2} z^{1/2}} K T_2^{0.383} \rho_2^{1/2} V_2^{2.39} \quad (Btu/ft^2/sec) \qquad (12)$$

where

$$K = \frac{5}{0.85 M_2^2} \left(1 - \frac{T_W}{T_2}\right) \qquad (13)$$

and

$$1 \leq M_2 \leq 7$$

The wetted surface distance term, z, in the approximate Van Driest equation requires some description. As stated before, space impingement flow on the flat plate is divided into two regions: the normal shock region and the oblique shock region. The distance, z, is measured from the end of the normal shock region to the point of interest.

[1] References 8 and 9

RESULTS

The results of the isentropic and Newtonian surface pressure predictions are compared in Figure 6 to the data obtained in the high-vacuum plume impingement test.[1] This figure shows that the agreement in absolute value is only fair, and that no conclusion can be reached as to whether isentropic or Newtonian pressure theory should be used for other calculations.

It is difficult to place an accuracy on the pressure data, because in nearly all the cases the data were recorded at less than 10 percent of the full range of the transducer. The fact that the shape of the data distribution agrees well with the predicted pressures, indicates that either method can be used to obtain a good approximation of the pressure distribution due to exhaust flow field impingement on a flat plate in space.

The centerline heating rate correlation is presented in Figures 7 through 11. These figures show that in spite of all of the assumptions made leading to the final correlations, the agreement between data and prediction is good.

It is noted that as the flow distance, z, in the oblique shock region, approaches zero, the calculated heating rate goes to infinity. Thus the correlation deviates from the measured data in this region. It appears from the data presented that the correlating equation is adequate for $z \geq 0.1$ foot.

---

[1] Reference 1

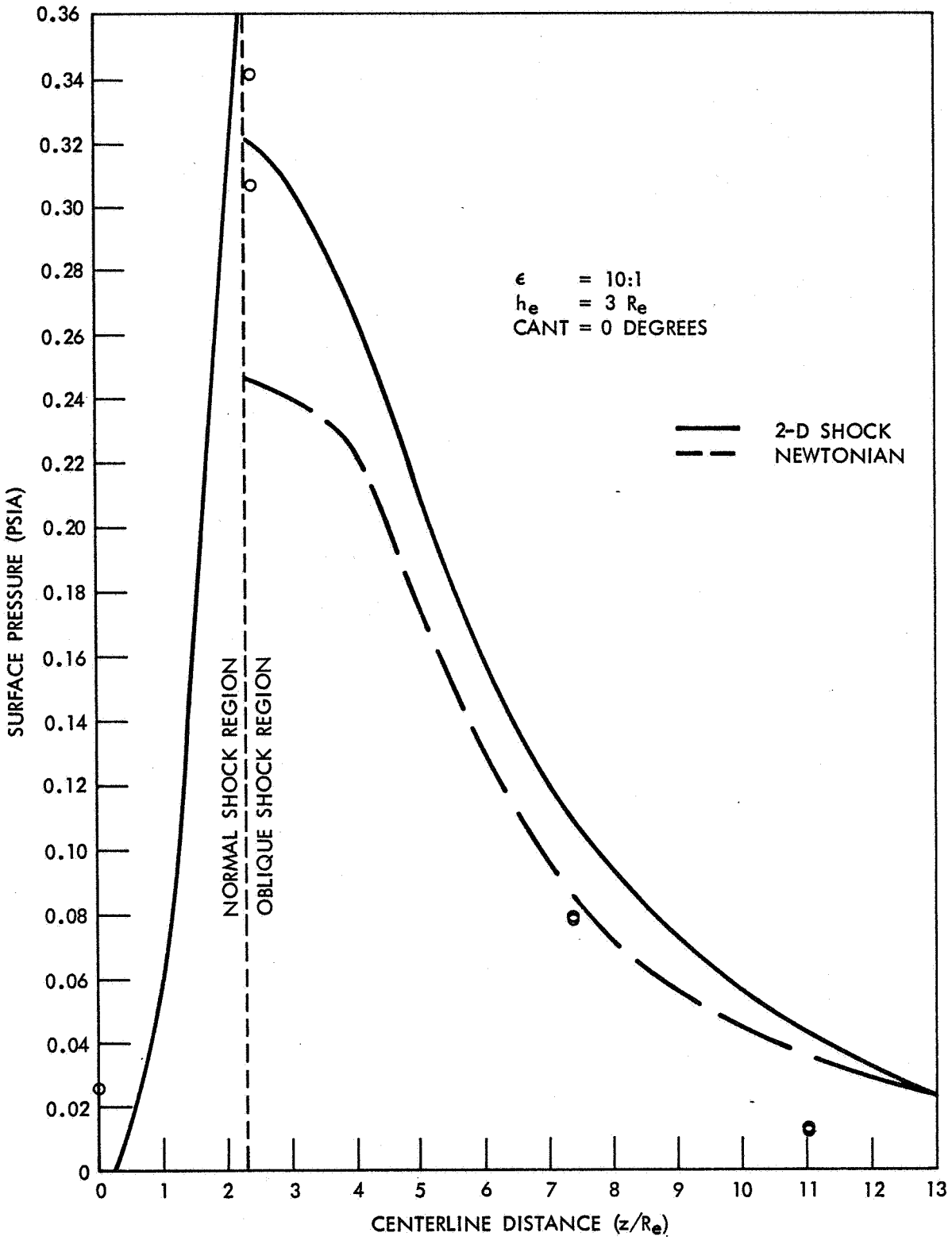

Figure 6. Surface Pressure Distribution, Service Module RCS Plume Impingement Test, ϵ= 10:1

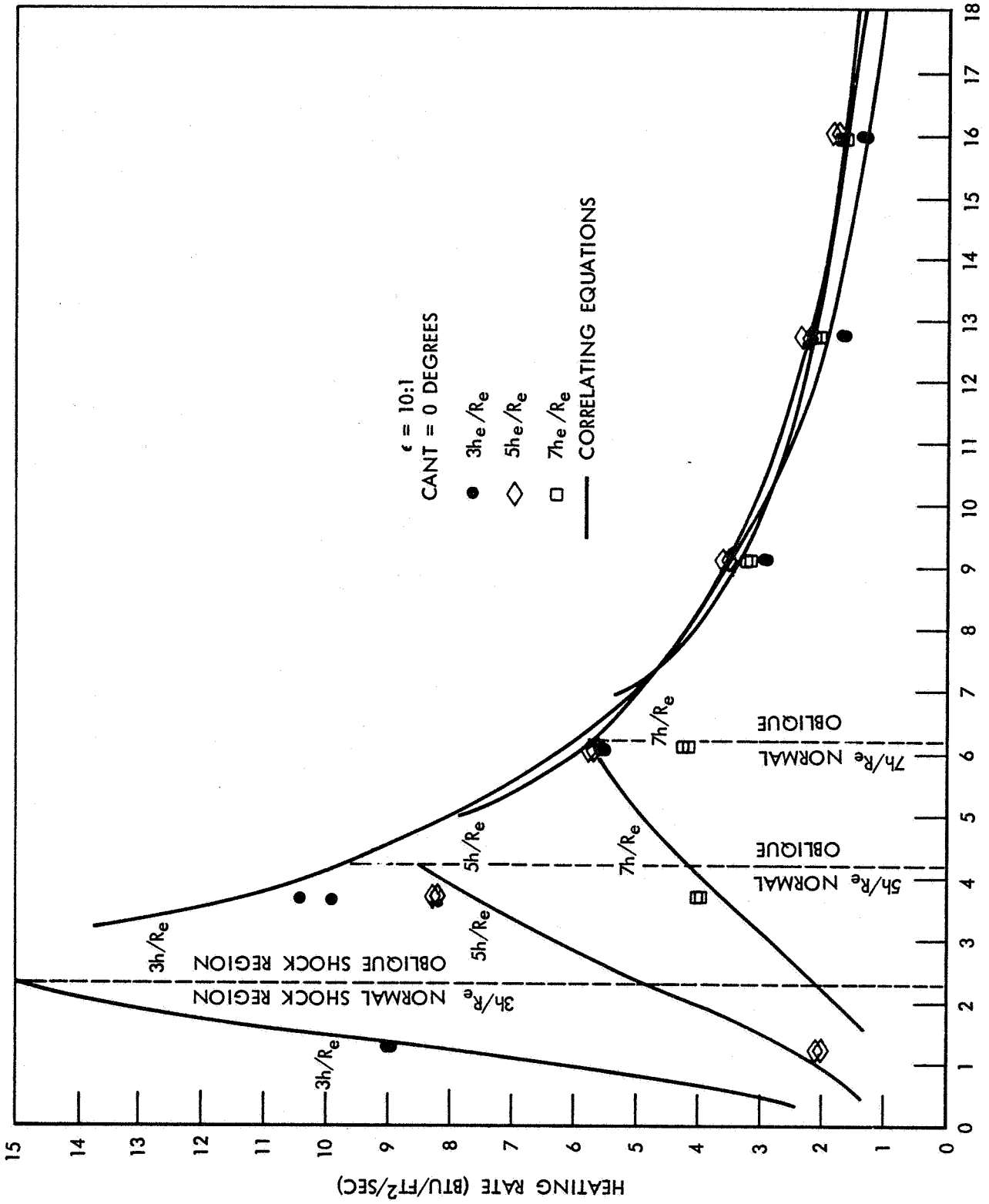

Figure 7. Heat Flux Distribution, Service Module RCS Plume Impingement Test, ϵ = 10:1

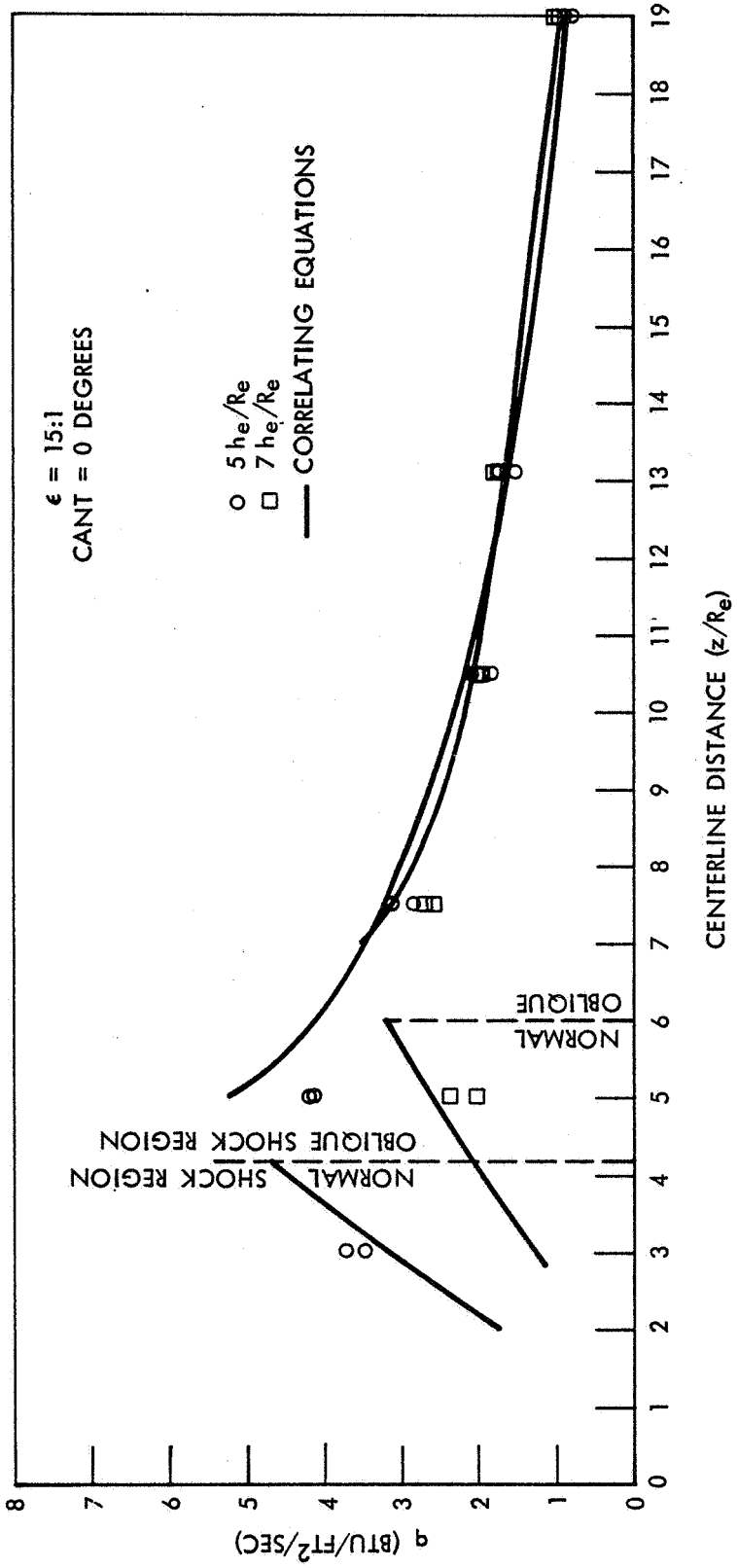

Figure 8. Heat Flux Distribution, Service Module RCS Plume Impingement Test, ϵ = 15:1

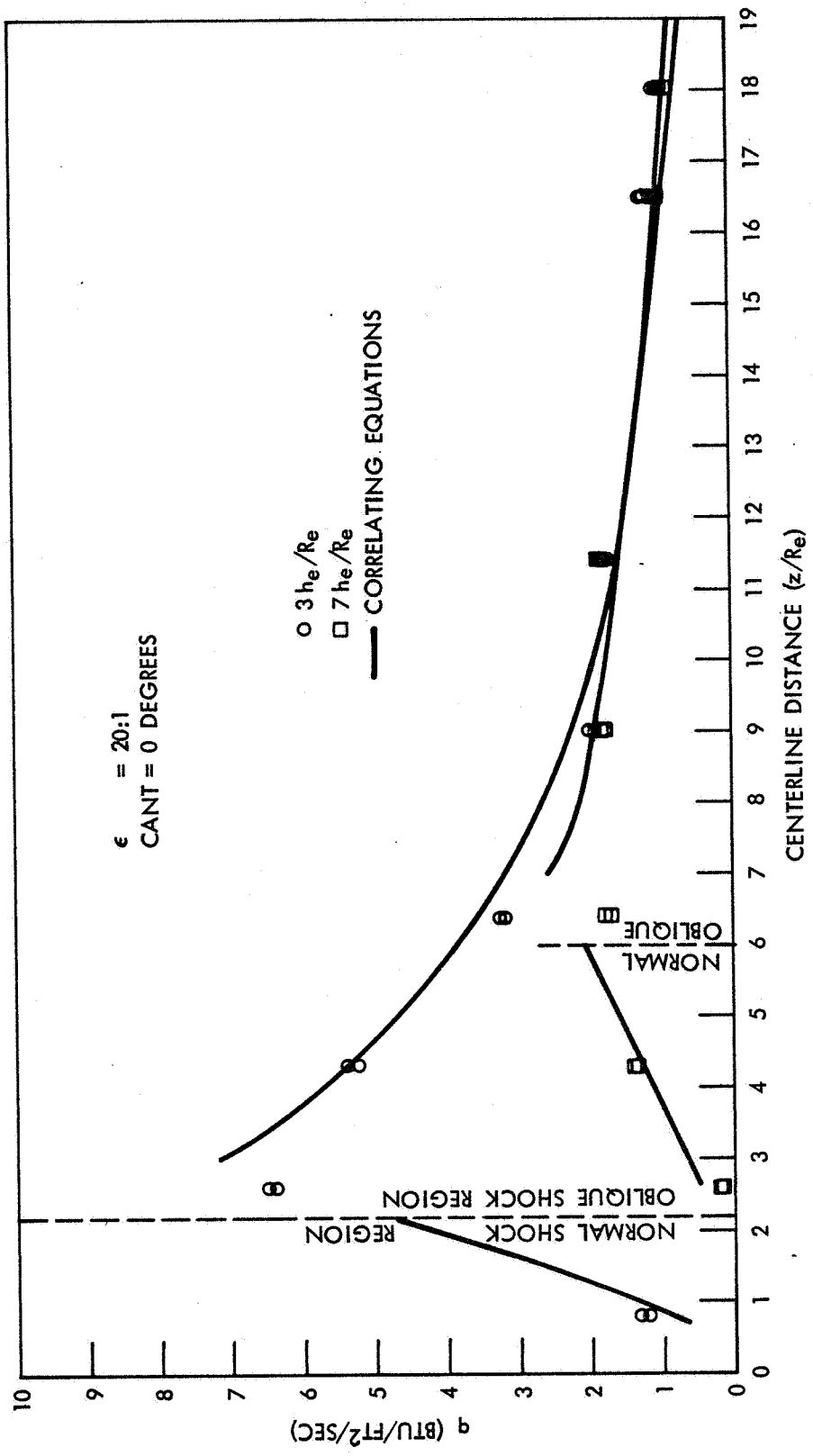

Figure 9. Heat Flux Distribution, Service Module RCS Plume Impingement Test, ε = 20:1

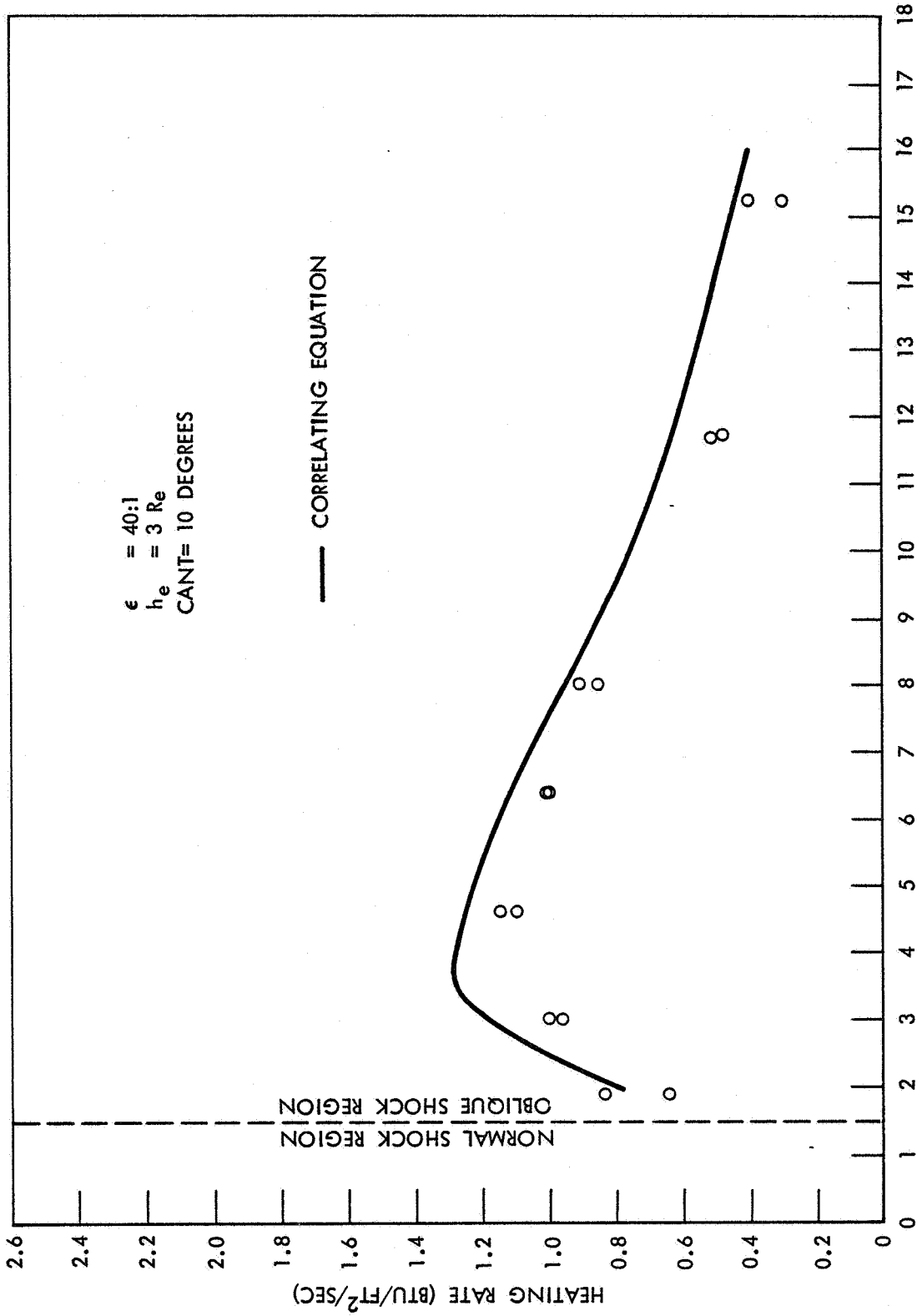

Figure 10. Heat Flux Distribution, Service Module RCS Plume Impingement Test, Service Module Design Case, ϵ= 40:1

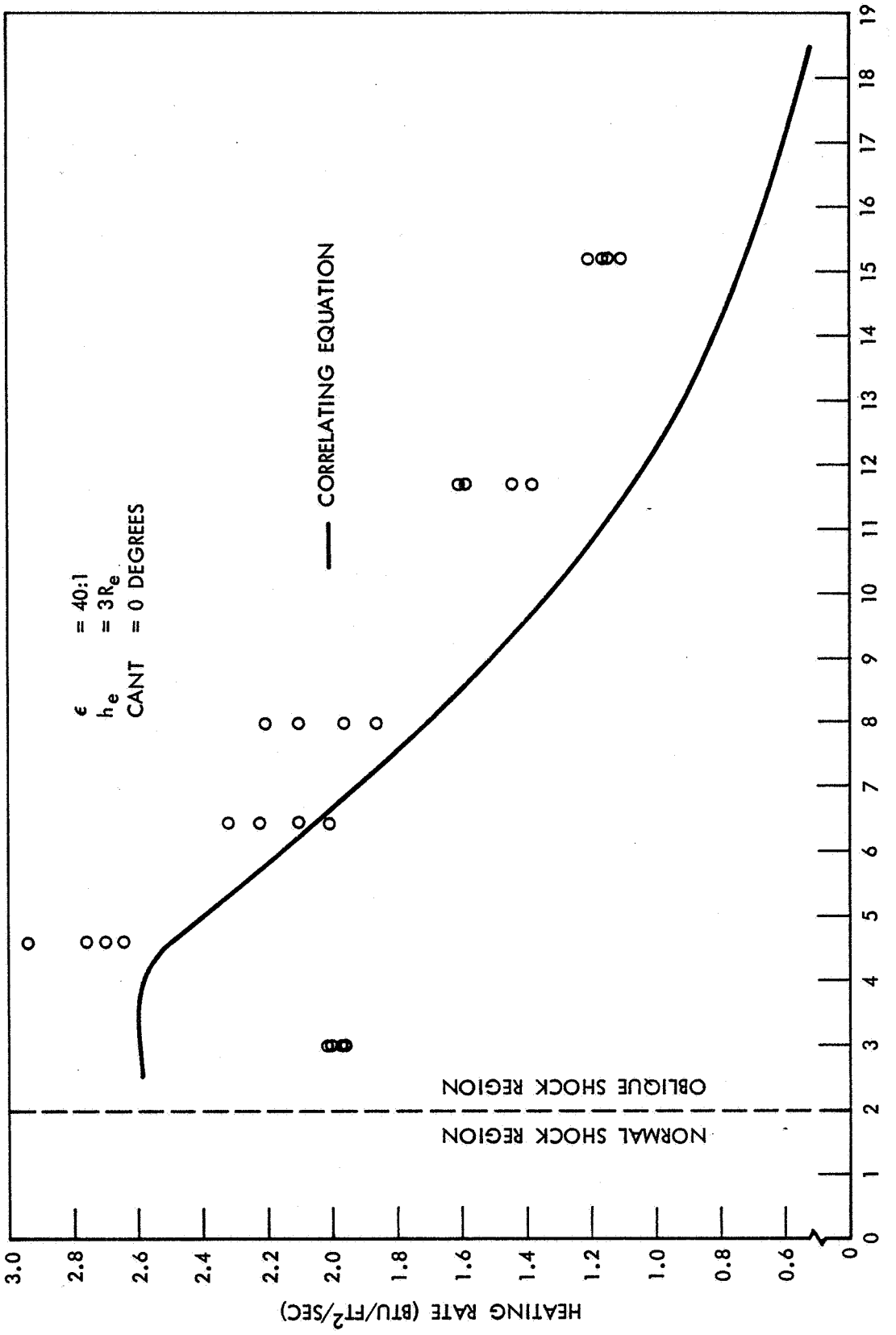

Figure 11. Heat Flux Distribution, Service Module RCS Plume Impingement Test, ϵ = 40:1

CONCLUSIONS

A method has been described for predicting heating rates and surface pressures resulting from a space exhaust plume impinging on a flat plate. In addition, the following assumptions have been verified:

1. Space exhaust impingement effects on surfaces can be obtained in Earth-bound vacuum chambers.

2. The local impingement properties inside the boundary shock of an exhaust flow field do not vary significantly over many orders of magnitude in ambient pressure.

3. At least for the engine tested, the highly underexpanded exhaust flow field from a contoured nozzle is adequately predicted for impingement analyses with the method of characteristics using constant exit plane properties at the nozzle exit.

REFERENCES

1. Piesik, E.T. High-Vacuum Plume Impingement Test Report. NAA S&ID, SID 63-1520 (25 Feb. 1964).

2. Wang, C.J., and J.B. Peterson. Spreading of Supersonic Axially Symmetric Nozzles. Ramo-Wooldridge Corp., GM-TR-175 (16 May 1957).

3. Bauer, R.C., and R.L. Schlumpf. Experimental Investigation of Free Jet Impingement on a Flat Plate. AEDC-TN-60-223 (March 1961).

4. Vick, A.R., and E.H. Andrews, Jr. An Experimental Investigation of Highly Underexpanded Free Jets Impinging Upon a Parallel Flat Surface. NASA TN-D2326 (June 1964).

5. Margolin, E.L., and E. Welch. Final Report—Single Nozzle Jet Plume Test in the Rocket Nozzle Test Facility. NAA S&ID, SID 63-426 (6 May 1963).

6. Kemp, N.H., and F.R. Riddell. "Heat Transfer to Satellite Vehicles Reentering the Atmosphere," Jet Propulsion, Vol. 27 (Feb. 1957), pp. 132-137.

7. Walker, S.C., C.L. Pratt, and F.H. Gaudmight. Integrated Back-Pack Maneuvering Unit Propulsion Study and Exhaust Plume Heating Analysis. ASD-TDR-63-729 (Sept. 1963).

8. Van Driest, E.R. Investigation of Laminar Boundary Layer in Compressible Fluids Using the Crocco Method. NACA TN 2597 (1952).

9. Harthun, M.H. "Methods and Procedures for Aerodynamic Heating Solutions," Aerodynamic Heating Manual, Vol. II, NAA Missile Division, ATS/60-167 (30 Sept. 1960).

APPENDIX

SYMBOLS

a	Speed of sound (ft/sec)
A	Area
g	Acceleration of gravity (32.2 ft/sec^2)
h	Distance from the point of interest perpendicular to the nozzle centerline
H	Enthalpy at the edge of the boundary layer
M	Mach number
P	Pressure (psia)
R	Gas constant (lb-ft/ft °R)
R_e	Nozzle exit radius (ft)
T	Temperature (R)
V	Velocity (ft/sec)
$\dot{W}$	Propellant flow rate (lb/sec)
z	Surface flow distance (ft)
ρ	Density (lb/ft^3)
γ	Specific heat ratio
θ_n	Nozzle half angle at exit plane
ζ	Efficiency
α	Impingement angle degrees
ϵ	Area ratio (A_e/A_t)

SUBSCRIPTS

1	Static value upstream of shock
1D	One dimensional
2	Static value downstream of shock
∞	Ambient
e	Exit
s	Surface
SL	Sea-level air
t	Total
W	Wall